

Article

Near-Infrared Absorbing Molecule Based on Triphenylamine Radical Cation with Extended Homoaryl π -System

Masafumi Yano ^{1,*}, Kohei Tamada ¹, Misaki Nakai ¹, Koichi Mitsudo ² and Yukiyasu Kashiwagi ³

¹ Faculty of Chemistry, Material and Bioengineering, Kansai University, 3-3-35 Yamate-cho, Suita 564-8680, Japan; k272417@kansai-u.ac.jp (K.T.); nakai@kansai-u.ac.jp (M.N.)

² Division of Applied Chemistry, Graduate School of Natural Science and Technology, Okayama University, 3-1-1 Tsushima-naka, Kita-ku, Okayama 700-8530, Japan; mitsudo@okayama-u.ac.jp

³ Osaka Research Institute of Industrial Science and Technology, 1-6-50 Morinomiya, Joto-ku, Osaka 536-8553, Japan; kashiwagi@orist.jp

* Correspondence: myano@kansai-u.ac.jp; Tel.: +81-6-6368-0751

Abstract: Four triphenylamines with extended π -systems were synthesized. Cyclic voltammetry (CV) measurements showed that they gave radical cations, which are stable in solution. Radical cations obtained upon one electron chemical oxidation showed strong absorption in the near-infrared region. The radical cations of the naphthalene-substituted derivatives show a maximum absorption wavelength above 1000 nm and are classified as NIR-II dyes. Molecular design rules of novel near-infrared absorbing dyes are described.

Keywords: triarylamines; radical cation; near infrared absorption; HOMO–SOMO transition



Citation: Yano, M.; Tamada, K.; Nakai, M.; Mitsudo, K.; Kashiwagi, Y. Near-Infrared Absorbing Molecule Based on Triphenylamine Radical Cation with Extended Homoaryl π -System. *Colorants* **2022**, *1*, 226–235. <https://doi.org/10.3390/colorants1020014>

Academic Editor: Anthony Harriman

Received: 21 April 2022

Accepted: 30 May 2022

Published: 2 June 2022

Publisher's Note: MDPI stays neutral with regard to jurisdictional claims in published maps and institutional affiliations.



Copyright: © 2022 by the authors. Licensee MDPI, Basel, Switzerland. This article is an open access article distributed under the terms and conditions of the Creative Commons Attribution (CC BY) license (<https://creativecommons.org/licenses/by/4.0/>).

1. Introduction

Near-infrared light is located between the visible and infrared regions in the wavelength range (800 to 2500 nm). Near-infrared absorbing dyes have absorption that shows strong optical absorption based on the charge transfer transition of organic dyes or metal complexes [1,2]. Among the near-infrared absorbing compounds containing cyanine dyes with extended polymethine skeletons are phthalocyanine dyes with aluminum or zinc at the center, various naphthalocyanine compounds, nickel dithiolenes complexes with planar tetracoordinate structures, squarylium dyes, quinone compounds, azo compounds, and so on [3–8]. The application of these dyes will allow us to develop a wide range of products in various optical fields such as security marking, lithography, optical recording media, and optical filters [1]. In the field of plate-making materials using laser light, high sensitivity to laser light with wavelengths longer than 700 nm is a growing demand, and excellent solubility in common organic solvents and heat resistance are also required for near-infrared absorbing compounds. Furthermore, in order to increase the efficiency of photovoltaic power generation, it is desirable to make effective use of the near-infrared light contained in sunlight; therefore, the development of materials that efficiently absorb near-infrared light is essential. On the other hand, the near-infrared luminescence phenomenon is expected to be applied to biomaterials for chemotherapy and the imaging of deep tissues in the body. Triphenylamines (TPAs) having various substituents at their para positions are widely known to give the corresponding very stable cation radicals upon chemical or electrochemical one-electron oxidation [9,10]. In the neutral state, tri-*p*-tolylamine (**1**) has an absorption around 300 nm due to the HOMO–LUMO transition, but no absorption in the visible region (Figure 1a). One-electron oxidation of **1** gives the stable blue radical cation **1**^{•+}, which has an absorption at 675 nm due to the HOMO–SOMO transition (Figure 1b) [11]. This absorption is characteristic of organic radicals. Although **1**^{•+} has only three aromatic rings, it can absorb light at wavelengths near the boundary between visible light and near-infrared light.

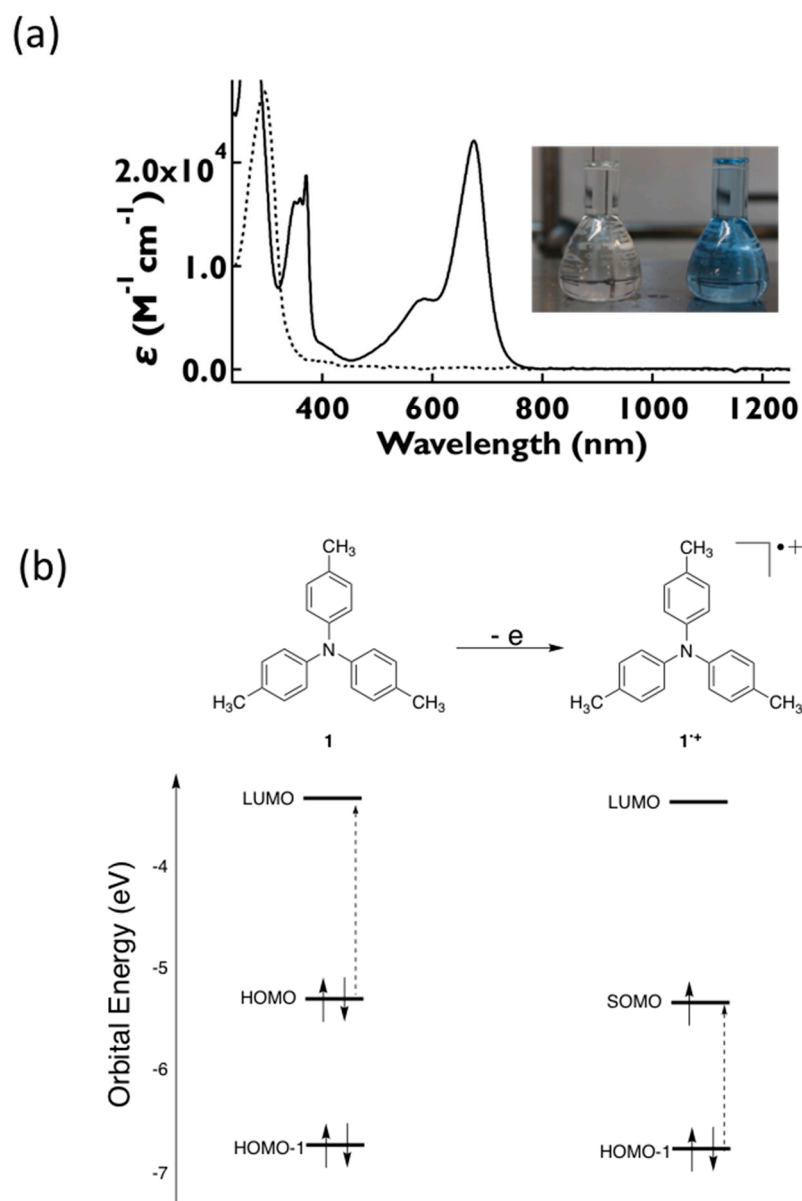
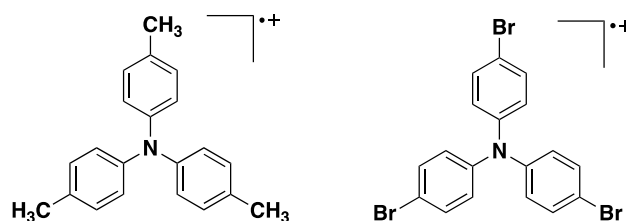


Figure 1. (a) Absorption spectra of **1** before (dotted line) and after oxidation with 10 equivalents of SbCl_5 (solid line) in dichloromethane at room temperature, $[\mathbf{1}] = 1 \times 10^{-5} \text{ M}$. Inset: dichloromethane solution of **1** in the absence (left) and presence of 10 equivalents of SbCl_5 (right), $[\mathbf{1}] = 1 \times 10^{-5} \text{ M}$. (b) Molecular orbital energy levels of **1** and **1** $^{\bullet+}$.

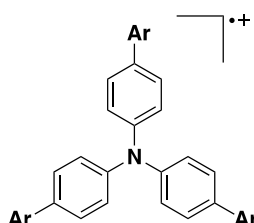
By taking advantage of this property, TPA electrochromic materials that can reversibly turn on and off the color change in the visible light range have been reported [12–15]. If triphenylamines with an extended π -system can be synthesized and stable radical cations can be obtained upon one-electron oxidation, they will be promising precursors for near-infrared absorbing materials. Based on this hypothesis, we considered phenyl-(**2**) [16], 4-biphenyl (**3**) [17], 1-naphthyl (**4**) [18], and 2-naphthyl (**5**) [19] substituted triphenylamines as promising precursors for near-infrared absorption materials. One-electron oxidation of each of them is expected to produce absorption in the near-infrared region (Figures 2 and 3). Although these compounds have been investigated as luminescent or hole-transfer materials, their use as near-infrared absorbing materials has not been explored at all.

Well-known TPA radical cations



Absorption in the visible light region (around 650 nm)

This study



Absorption in the near-infrared light region (around 1000 nm)

Figure 2. Representative stable TPA radical cations and this study.

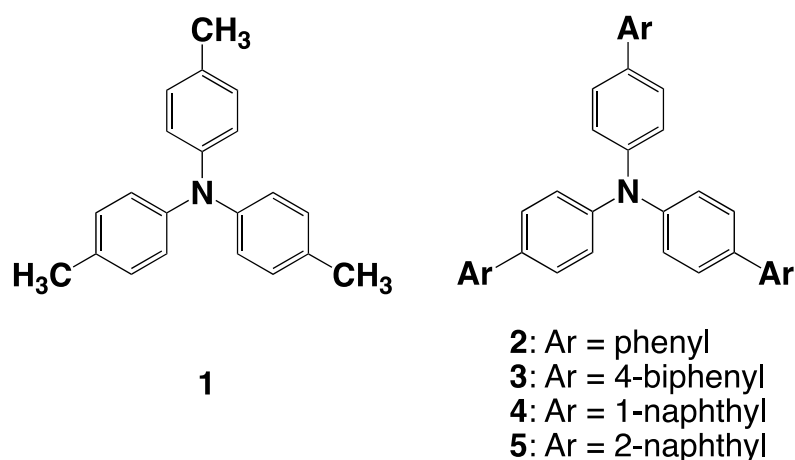


Figure 3. Structures of compounds 1–5.

2. Results and Discussion

2.1. Theoretical Calculations

In order to estimate whether radical cations $2^{\bullet+}$ – $5^{\bullet+}$ with extended π -systems have absorption in the near-infrared region, DFT calculations were carried out on compounds $1^{\bullet+}$ – $5^{\bullet+}$ at the UB3LYP/6-31G(d) level of theory with the polarizable continuum model, using dichloromethane as a solvent (Figure 4). The calculated HOMO–SOMO energy gap of $1^{\bullet+}$ is 1.60 eV, and $1^{\bullet+}$ is expected to have a maximum absorption at 633 nm in dichloromethane. Indeed, $1^{\bullet+}$ has a maximum absorption at 675 nm in dichloromethane [20], indicating the validity of this calculation method. The HOMO–SOMO energy gap of $2^{\bullet+}$ (1.28 eV) was smaller than that of $1^{\bullet+}$. The calculated maximum absorption wavelength of $2^{\bullet+}$ is 857 nm, which corresponds to the near-infrared region, indicating that the introduction of the phenyl group effectively would reduce the HOMO–SOMO energy gap. Furthermore, $3^{\bullet+}$ with biphenyl units is found to have a narrower SOMO–HOMO energy gap (1.12 eV) than $2^{\bullet+}$, suggesting a further long-wavelength shift. Compounds $4^{\bullet+}$ and $5^{\bullet+}$, extended

with 1- or 2-naphthyl groups, were found to have a HOMO–SOMO gap narrower than $2^{\bullet+}$. These results (see Supplementary Materials for more information on the results of DFT calculations) suggest that triphenylamine radical cations with an extended π -system by extra aromatic rings have absorption in the near-infrared region. These results prompted us to prepare 2–5 and investigate the properties of the corresponding radical cations $2^{\bullet+}$ – $5^{\bullet+}$.

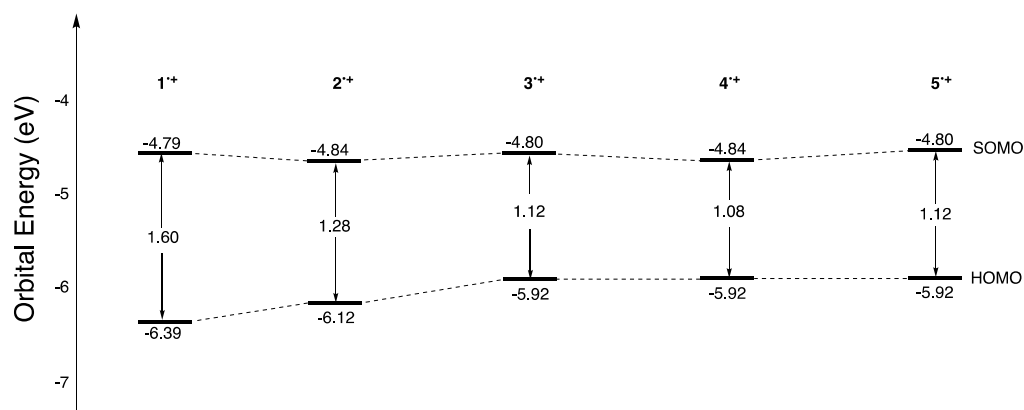
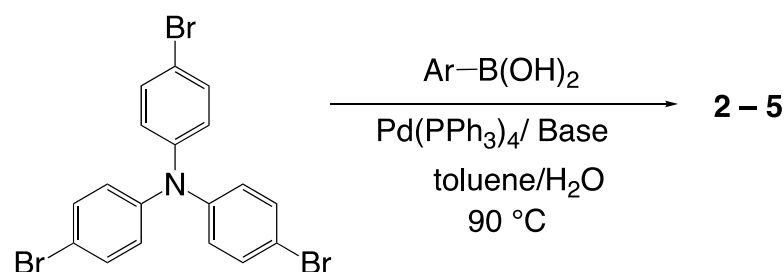


Figure 4. Molecular orbital energy levels of $1^{\bullet+}$ – $5^{\bullet+}$.

2.2. Synthesis

The synthetic route for 2–5 is depicted in Scheme 1. These compounds were synthesized in one step by modifying the previously reported method [18,19]. The corresponding aryl boronic acid was reacted with 4, 4', 4''-tribromotriphenylamine under Pd-catalyzed Suzuki coupling reaction conditions to give the target compound in a moderate yield (see Supplementary Materials for details).



Scheme 1. Synthesis of 2–5.

2.3. Solubility

In general, compounds with highly extended π -systems have low solubility in organic solvents [21]. However, to be employed in organic electronics, a solubility of more than 0.1 wt% is required in general organic solvents [22]. We examined the solubility of compounds 2–5 in several organic solvents. Compound 2 showed good solubility in dichloromethane, anisole, and toluene. On the other hand, 2 was almost insoluble in ethyl acetate. Compound 3, which has an extended π -system with *p*-phenylene units, has a very low solubility compared to 2. Among the four compounds examined in this study, 4 showed the highest solubility. A comparison of the solubility of 4 and 5 in a structural isomer relationship showed that 4 was about 10 times more soluble than 5 in various organic solvents (see Supplementary Materials for details for the solubilities of 2–5 in various organic solvents).

2.4. Crystal Structures of 4 and 5

In order to clarify the difference in solubility between 4 and 5, the crystal structures of these two compounds were compared. The crystal structure of 4 was previously reported

by us [23]. In this study, we prepared single crystals of **5** and clarified their crystal structures [24]. The crystal structures of **4** and **5** are shown in Figure 5. In compound **4**, the dihedral angles of the naphthyl and *p*-phenylene groups are 48.8–56.2°. On the other hand, those for **5** are 16.6–40.3°. The 1-naphthyl and *p*-phenylene groups in compound **4** are twisted more significantly by steric hindrance. This prevents tight intermolecular packing and is thought to result in high solubility.

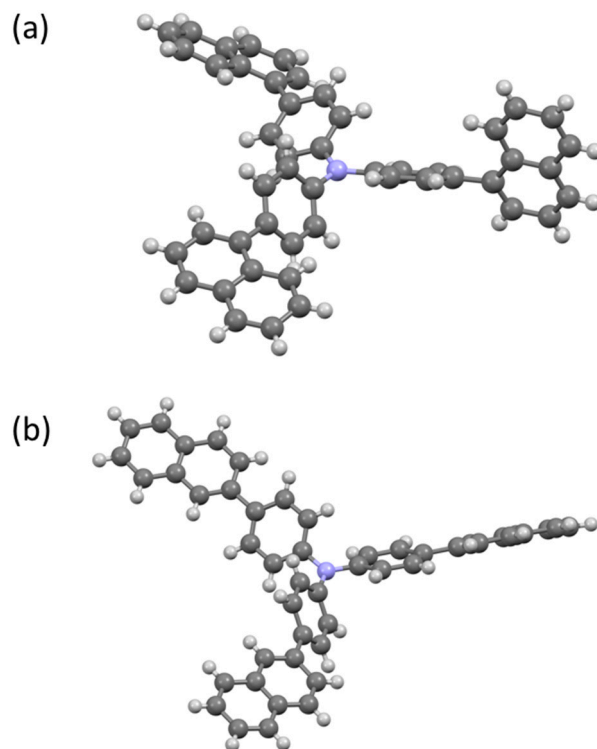


Figure 5. Crystal structures of (a) **4** and (b) **5**.

2.5. Cyclic Voltammetry Measurements

Cyclic voltammetry measurements were performed to clarify the electrochemical properties of **2–5** at room temperature in dichloromethane, using 0.1 M tetra-*n*-butylammonium hexafluorophosphate (Bu_4NPF_6) as the supporting electrolyte. On an anodic sweep, **2** showed a reversible redox wave ($E^0 = 0.42$ V vs. Fc/Fc^+). This was attributed to the one-electron oxidation of the triarylamine site (Figure 6).

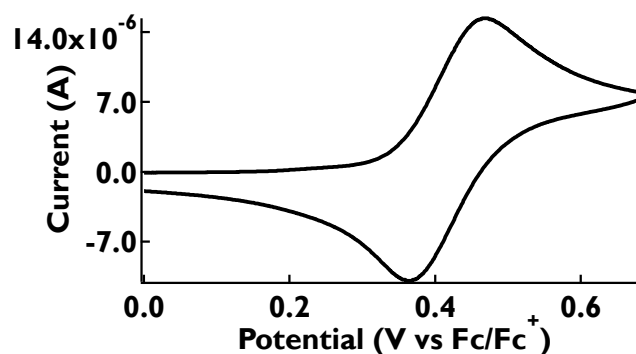


Figure 6. Cyclic voltammogram of **2** in dichloromethane (1×10^{-3} M) with 0.1 M Bu_4NPF_6 as a supporting electrolyte. The scan rate was 100 mV/s.

The shape of the voltammogram did not change even after 10 cycles at a sweep rate of 25 mV/s (Figure S8). This result indicates that the radical cation $\mathbf{2}^{\bullet+}$ is very stable

in solution. Similarly, compound **3** showed reversible one-electron oxidation transfer ($E^0 = 0.42$ V vs. Fc/Fc⁺). Similarly, the voltammograms of **3–5** were reversible, respectively (see Supplementary Materials for details). The redox potentials and HOMO energy levels by DFT calculations for compounds **1–5** are shown in Table 1. The value of the redox potentials E^0 showed good agreement with the values of the HOMO energy level obtained from the DFT calculations. Compounds **1–5** in solution were found to give stable radical cations at room temperature. With these results, we set out to study their absorption spectra.

Table 1. Electrochemical data for **1–5** with calculated E_{HOMO} .

Compound	E^0 (V vs. Fc/Fc ⁺)	E_{HOMO} (eV)
1	0.33	−4.87
2	0.42	−4.97
3	0.42	−4.95
4	0.47	−5.00
5	0.42	−4.96

2.6. Absorption and Fluorescence Spectra of the Neutral Species, **1–5**

The absorption and fluorescence spectra of compounds **1–5** in a neutral state were studied in dichloromethane. The absorption and fluorescence spectra of **2** are shown in Figure 7. A large absorption appears at 344 nm. DFT calculations revealed that this absorption was due to the HOMO–LUMO and HOMO–LUMO+1 transitions. Similar studies were conducted for compounds **3–5** (see Supplementary Materials for details). The experimental and DFT calculated absorption spectra of compounds **1–5** are summarized in Table 2. The peak shifted to the long wavelength side as an extension of the π -system. The experimental and calculated values were in good agreement. Upon excitation at 344 nm, **2** showed blue emission at 416 nm. As the π system was extended, the emission wavelength shifted to the longer wavelength side. The experimental fluorescence spectra of compounds **1–5** are also summarized in Table 2 (see also Supplementary Materials).

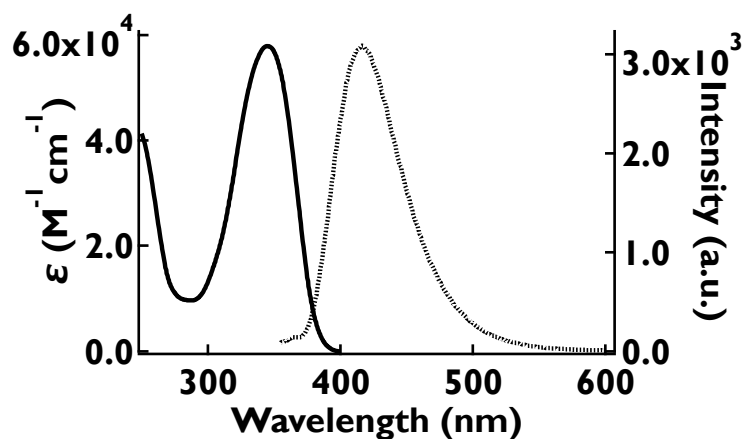


Figure 7. UV-Vis (solid line) and fluorescence emission (dotted line) spectra of **2** in dichloromethane. The concentration was 1×10^{-5} M for UV-Vis and 1×10^{-6} M for fluorescence emission spectra.

Table 2. The experimental and calculation results for the absorption spectra of 1–5.

Compound	Absorption Spectra			Fluorescence Spectra
	Obsd.		Calcd.	Obsd.
	λ_{max} (nm)	$\log \epsilon$	λ_{max} (nm)	λ_{max} (nm)
1	294	4.43	326	-
2	344	4.78	363	416
3	361	4.71	390	442
4	341	4.65	379	437
5	363	4.84	393	440

2.7. UV-Vis-NIR Absorption and Fluorescence Spectra of the Oxidized Species, $1^{\bullet+}$ – $5^{\bullet+}$

The UV-Vis-NIR spectrum of the oxidized species $2^{\bullet+}$ was examined in dichloromethane (Figure 8). When 10 equivalents of $SbCl_5$ were added to the solution of **2**, the color of the solution changed to a light yellowish green, indicating the formation of oxidized species $2^{\bullet+}$. In agreement with the results of TD-DFT calculations, new absorptions appeared at 420 and 862 nm (Figure S18). TD-DFT calculations suggest that this near-infrared absorption at 862 nm was due to the HOMO to SOMO transition.

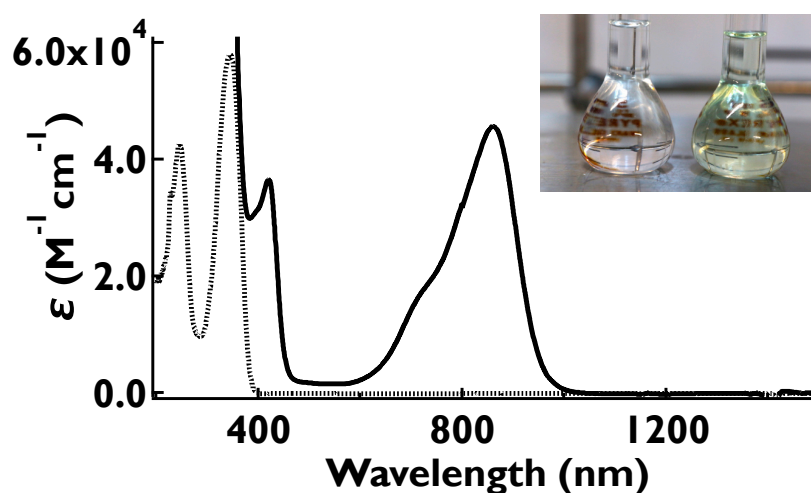


Figure 8. Absorption spectra of **2** before (dotted line) and after oxidation with 10 equivalents of $SbCl_5$ (solid line) in dichloromethane at room temperature, $[2] = 1 \times 10^{-5}$ M. Inset: dichloromethane solution of **2** in the absence (left) and presence of 10 equivalents of $SbCl_5$ (right), $[2] = 1 \times 10^{-5}$ M.

This absorption did not change at all over 15 min at room temperature under nitrogen atmosphere (Figure 9). Compounds **3**–**5** were studied in the same way (see Supplementary Materials for details). When 10 equivalents of $SbCl_5$ were added to the solution of **3**, the color of the solution changed to yellow (Figure S12) and new absorptions appeared at 991 nm (Figure S15). The maximum absorption peak in the near-infrared region of $3^{\bullet+}$ was shifted to the longer wavelength side by 129 nm compared to that of $2^{\bullet+}$. Compounds $4^{\bullet+}$ and $5^{\bullet+}$ with naphthalene rings showed maximum absorption at 1071 and 1028 nm, respectively (Figures S16 and S17). The results of the absorption spectra of $1^{\bullet+}$ – $5^{\bullet+}$ are summarized in Table 3.

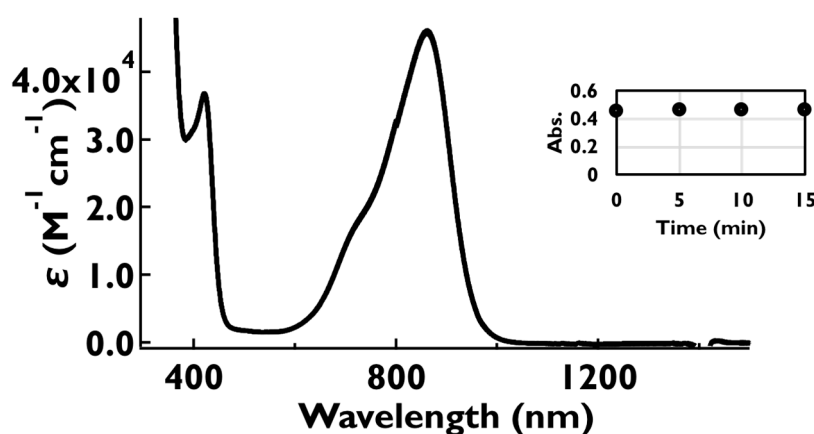


Figure 9. Time course of UV-Vis absorption spectra of **2** with 10 equivalents of SbCl_5 in dichloromethane at room temperature recorded every 5 min. The initial concentration of **2** was 1×10^{-5} M. Inset: time course of the peak intensity at 862 nm.

Table 3. Spectroscopic properties and DFT calculation results for $1^{\bullet+}$ – $5^{\bullet+}$.

	Absorption Spectra			DFT Calculation		
	Obsd.		Calcd.	HOMO (eV)	SOMO (eV)	ΔE (eV)
	λ_{max} (nm)	$\log \epsilon$	λ_{max} (nm)			
1^{•+}	675	4.34	633	−6.39	−4.79	1.60
2^{•+}	862	4.66	857	−6.12	−4.84	1.28
3^{•+}	991	4.46	1113	−5.92	−4.80	1.12
4^{•+}	1071	4.46	1349	−5.92	−4.84	1.08
5^{•+}	1028	4.56	1244	−5.92	−4.80	1.12

Among the four compounds, **2**–**5**, examined in this study, **4**, with its twisted structure, exhibited the highest solubility. Furthermore, among the four corresponding radical cations, $2^{\bullet+}$ – $5^{\bullet+}$, the absorption peak of $4^{\bullet+}$ was shifted to the longest wavelength region. This indicates that the 1-naphthyl group is a promising substituent for both high solubility and effective π -system extension in the design of TPA derivatives. This oxidized species $4^{\bullet+}$ was reduced by ascorbic acid to regenerate **4** almost quantitatively (see Figures S29 and S30 for details). Fluorescence emission spectra of **2**–**5** and their oxidized species in dichloromethane are shown in Figures S31–S34. Upon the addition of 10 equivalents of SbCl_5 , the emission was quenched almost completely.

3. Conclusions

Four triaryl amines with extended π -systems were investigated as precursors for near-infrared absorbing materials. CV measurements and chemical oxidation studies revealed that they gave radical cations that were stable in solution. These radical cations were found to have a significant absorption in the near-infrared region (around 1000 nm). Especially, the two radical cations with naphthalene, $4^{\bullet+}$ and $5^{\bullet+}$, showed maximum absorption wavelengths above 1000 nm and were classified as NIR-II dyes, which are expected to be applied in various fields [4–6]. DFT calculations showed that this absorption was due to the HOMO–SOMO transition of the radical cation. The NIR-II dyes reported so far have complicated structures, and their syntheses have been complex. On the other hand, the derivatives reported in this study can be easily synthesized in one step from commercially available reagents. Various substituents can be easily introduced into the triarylamine core. It is expected that the absorption of radical cations can be shifted to longer wavelengths by further expansion of the π -system. Following this molecular design rule, studies of various π -extended triaryl amines are underway in our laboratory.

Supplementary Materials: The following supporting information can be downloaded at <https://www.mdpi.com/article/10.3390/colorants1020014/s1>. Synthesis, DFT calculations, solubility test, cyclic voltammetry, absorption and emission spectra of the neutral or oxidized species, and reduction in the radical cation $4^{\bullet+}$ with ascorbic acid. Fluorescence spectra, ^1H and ^{13}C spectra, and ESR spectra [18,19,25–31].

Author Contributions: Idea and writing, M.Y.; organic synthesis and physical properties' measurement, K.T.; UV spectroscopy and fluorescence measurement, M.N.; idea and DFT calculation, K.M.; idea, writing, and IR measurement, Y.K. All authors have read and agreed to the published version of the manuscript.

Funding: This research received no external funding.

Acknowledgments: The authors would like to thank Hitoshi Ishida, Kansai University, for the measurements of UV-Vis-NIR and spectra, Tatsuo Yajima, Kansai University, for the measurements of ESR spectra, and Toshiyuki Iwai, Osaka Research Institute of Industrial Science and Technology, for the measurements of HRMS.

Conflicts of Interest: The authors declare no conflict of interest.

References and Notes

1. Wang, Z. *Near-Infrared Organic Materials and Emerging Applications*, 1st ed.; CRC Press: Boca Raton, FL, USA, 2013.
2. Matsuoka, M. *Infrared Absorbing Dyes (Topics in Applied Chemistry)*; Springer: Berlin/Heidelberg, Germany, 1990; ISBN 0306434784.
3. Fabian, J.; Nakazumi, H.; Matsuoka, M. Near-infrared absorbing dyes. *Chem. Rev.* **1992**, *92*, 1197–1226. [[CrossRef](#)]
4. Rao, R.S.; Suman; Singh, S.P. Near-Infrared (>1000 nm) Light-Harvesters: Design, Synthesis and Applications. *Chem. A Eur. J.* **2020**, *26*, 16582–16593. [[CrossRef](#)] [[PubMed](#)]
5. Li, L.; Dong, X.; Li, J.; Wei, J. A short review on NIR-II organic small molecule dyes. *Dye. Pigment.* **2020**, *183*, 108756. [[CrossRef](#)]
6. Li, B.; Zhao, M.; Zhang, F. Rational Design of Near-Infrared-II Organic Molecular Dyes for Bioimaging and Biosensing. *ACS Mater. Lett.* **2020**, *2*, 905–917. [[CrossRef](#)]
7. Qi, J.; Qiao, W.; Wang, Z.Y. Advances in Organic Near-Infrared Materials and Emerging Applications. *Chem. Rec.* **2016**, *16*, 1531–1548. [[CrossRef](#)]
8. Sun, Z.; Wu, J. Higher order acenes and fused acenes with near-infrared absorption and emission. *Aust. J. Chem.* **2011**, *64*, 519–528. [[CrossRef](#)]
9. Seo, E.T.; Nelson, R.F.; Fritsch, J.M.; Marcoux, L.S.; Leedy, D.W.; Adams, R.N. Anodic Oxidation Pathways of Aromatic Amines. Electrochemical and Electron Paramagnetic Resonance Studies. *J. Am. Chem. Soc.* **1966**, *88*, 3498–3503. [[CrossRef](#)]
10. Nelson, R.R.; Adams, R.N. Anodic oxidation pathways of substituted triphenylamines. II. Quantitative studies of benzidine formation. *J. Am. Chem. Soc.* **1968**, *90*, 3925–3930. [[CrossRef](#)]
11. Nelson, R.F.; Philp, R.H. Electrochemical and spectroscopic studies of cation radicals. 4. Stopped-flow determination of triarylaminium radical coupling rate constants. *J. Phys. Chem.* **1979**, *83*, 713–716. [[CrossRef](#)]
12. Quinton, C.; Alain-Rizzo, V.; Dumas-Verdes, C.; Miomandre, F.; Audebert, P. Tetrazine-triphenylamine dyads: Influence of the nature of the linker on their properties. *Electrochim. Acta* **2013**, *110*, 693–701. [[CrossRef](#)]
13. Golba, S.; Starczewska, O.; Idzik, K. Electrochemical and spectrophotometric properties of polymers based on derivatives of di- and triphenylamines as promising materials for electronic applications. *Des. Monomers Polym.* **2015**, *18*, 770–779. [[CrossRef](#)]
14. Yen, H.-J.; Liou, G.-S. Solution-processable triarylamine-based electroactive high performance polymers for anodically electrochromic applications. *Polym. Chem.* **2012**, *3*, 255–264. [[CrossRef](#)]
15. Yan, Y.; Sun, N.; Jia, X.; Liu, X.; Wang, C.; Chao, D. Electrochromic and electrofluorochromic behavior of novel polyurea bearing oligoaniline and triphenylamine units. *Polymer* **2018**, *134*, 1–7. [[CrossRef](#)]
16. Vamvounis, G.; Shaw, P.E.; Burn, P.L. Design protocols in triarylamine cored dendrimer-based explosive sensors. *J. Mater. Chem. C* **2013**, *1*, 1322–1329. [[CrossRef](#)]
17. Higuchi, A.; Ohnishi, K.; Nomura, S.; Inada, H.; Shirota, Y. Tri(biphenyl-4-yl)amine and tri(p-terphenyl-4-yl)amine as a novel class of molecules for amorphous molecular materials. *J. Mater. Chem.* **1992**, *2*, 1109–1110. [[CrossRef](#)]
18. Kwon, J.; Kim, M.K.; Hong, J.-P.; Lee, W.; Noh, S.; Lee, C.; Lee, S.; Hong, J.-I. 4,4',4''-Tris(4-naphthalen-1-yl-phenyl)amine as a multifunctional material for organic light-emitting diodes, organic solar cells, and organic thin-film transistors. *Org. Electron.* **2010**, *11*, 1288–1295. [[CrossRef](#)]
19. Kwon, J.; Kim, M.K.; Hong, J.-P.; Lee, W.; Lee, S.; Hong, J.-I. A Multifunctional Material Based on Triphenylamine and a Naphthyl Unit for Organic Light-Emitting Diodes, Organic Solar Cells, and Organic Thin-Film Transistors. *Bull. Korean Chem. Soc.* **2013**, *34*, 1355–1360. [[CrossRef](#)]
20. Amthor, S.; Noller, B.; Lambert, C. UV/Vis/NIR spectral properties of triarylaminines and their corresponding radical cations. *Chem. Phys.* **2005**, *316*, 141–152. [[CrossRef](#)]

21. Rim, Y.S.; Bae, S.; Chen, H.; De Marco, N.; Yang, Y. Recent Progress in Materials and Devices toward Printable and Flexible Sensors. *Adv. Mater.* **2016**, *28*, 4415–4440. [[CrossRef](#)]
22. Okamoto, T.; Mitsui, C.; Yamagishi, M.; Nakahara, K.; Soeda, J.; Hirose, Y.; Miwa, K.; Sato, H.; Yamano, A.; Matsushita, T.; et al. V-shaped organic semiconductors with solution processability, high mobility, and high thermal durability. *Adv. Mater.* **2013**, *25*, 6392–6397. [[CrossRef](#)]
23. Yano, M.; Kashiwagi, Y.; Inada, Y.; Hayashi, Y.; Mitsudo, K.; Kubono, K. Crystal structure of tris [4-(naphthalen-1-yl)phenyl]amine. *Acta Crystallogr. Sect. E Crystallogr. Commun.* **2020**, *76*, 1649–1652. [[CrossRef](#)] [[PubMed](#)]
24. CCDC 2164002 (5) contains the supplementary crystallographic data for this paper. These data can be obtained free of charge via www.ccdc.cam.ac.uk/data_request/cif, or by emailing data_request@ccdc.cam.ac.uk, or by contacting The Cambridge Crystallographic Data Centre, 12 Union Road, Cambridge CB2 1EZ, UK; fax: +44-1223-336033.
25. Wang, K.; Deng, Z.H.; Xie, S.J.; Zhai, D.D.; Fang, H.Y.; Shi, Z.J. Synthesis of arylamines and N-heterocycles by direct catalytic nitrogenation using N₂. *Nat. Commun.* **2021**, *12*, 248. [[CrossRef](#)]
26. Frisch, M.J.; Trucks, G.W.; Schlegel, H.B.; Scuseria, G.E.; Robb, M.A.; Cheeseman, J.R.; Scalmani, G.; Barone, V.; Mennucci, B.; Petersson, G.A.; et al. *Gaussian 09, Revision E.01*; Gaussian, Inc.: Wallingford, CT, USA, 2009.
27. Becke, A.D. Density-functional thermochemistry. III. The role of exact exchange. *J. Chem. Phys.* **1993**, *98*, 5648–5652. [[CrossRef](#)]
28. Lee, C.; Yang, W.; Parr, R.G. Development of the Colle-Salvetti correlation-energy formula into a functional of the electron density. *Phys. Rev. B* **1988**, *37*, 785–789. [[CrossRef](#)]
29. Becke, A.D. A new mixing of Hartree–Fock and local density-functional theories. *J. Chem. Phys.* **1993**, *98*, 1372–1380. [[CrossRef](#)]
30. Stephens, P.J.; Devlin, F.J.; Chabalowski, C.F.; Frisch, M.J. Ab Initio Calculation of Vibrational Absorption and Circular Dichroism Spectra Using Density Functional Force Fields. *J. Phys. Chem.* **1994**, *98*, 11623–11627. [[CrossRef](#)]
31. Tomasi, J.; Mennucci, B.; Cammi, R. Quantum Mechanical Continuum Solvation Models. *Chem. Rev.* **2005**, *105*, 2999–3093. [[CrossRef](#)] [[PubMed](#)]